OMAE 2006-92355

A STUDY OF LES MODELS FOR THE SIMULATION OF A TURBULENT FLOW AROUND A TRUSS SPAR GEOMETRY

Senu Sirnivas,
Technip USA, Houston, USA

O. Allain, S. Wornom, A. Dervieux
Societe Lemma, La Roquette, France

B. Koobus
University of Montpellier, France

ABSTRACT

A new generation of LES type model is used to simulate the flow around a Spar geometry. This new method involves a Variational Multiscale formulation, allowing better capture of the back scatter. This approach is well suited for flows where small scales transmit a notable amount of energy to larger ones. The flow simulation is compared with experimental data from a model test.

INTRODUCTION

Spar platforms have been in service in the Gulf of Mexico since 1996 for combinations of production, workover, and drilling applications. It resembles a cylinder and when exposed to a steady current, sheds vortices from one side to the other resulting in pressure oscillation, which causes Vortex Induced Motion (VIM) [1]. These inline and transverse vibrations are measured in experiments as the dimensionless amplitudes Y/D and X/D shown in Figure 1.
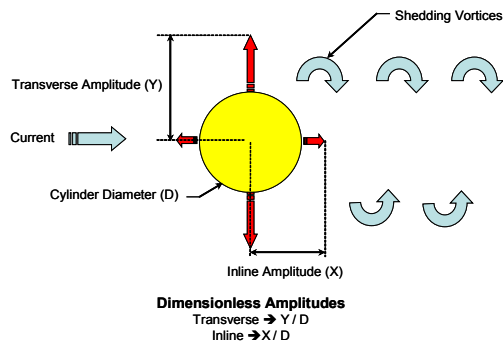

Figure 1: Dimensionless Amplitudes

VIM has serious consequences on fatigue of mooring and riser systems, and suppression is achieved through helical strakes, which disrupts the formation of vortex. Presently there is no analytical means of predicting the effectiveness of strake design other than resorting to long and costly experiments conducted in model basin. This paper explores an alternate approach using numerical methods in Computational Fluid Dynamics (CFD), currently being investigated by many researchers. Investigation of this approach is presented here by comparing the transverse vibration of a Truss Spar (Spar), selected from the direction which produced the largest vibrations in the experiment, for a range of currents.

Given the limitation to small computer clusters, the resulting mesh for this study is not feasible for Direct Numerical Simulation (DNS). Statistical models like Unsteady Reynolds-Averaged Navier-Stokes (URANS) produces insufficient information about turbulence, leading to poor overall predictions. However, due to mesh size limitations, this option might work well in some regions of the flow. The geometry of the Spar is complicated by helical strakes, chains, and fairleads on the hard tank, cross braces and heave plates in the truss section, and soft tank, which greatly influence its hydrodynamic characteristic.

Previous work using CFD with finite element techniques has been published on this subject [4] [5]. The studies show that vibration trends with respect to reduced velocities could be predicted well, but where significant response is observed in the experiment, significant over prediction results from CFD method. These investigations further demonstrate that small scale flow details, such as those arising at separation on strake edges, may inhibit large scale vortices. This tends to show that back-scatter energy transfer mechanism from small to large

scales must be accounted for and be preserved from the model's spurious dissipation as much as possible. This study is restricted to combining Boussinesq-based models, i.e. where Reynolds tensors are modeled by dissipative terms, the weight of which becomes of paramount importance. It explores Variationnal Multiscale (VMS) formulation.

EXPERIMENT

A Truss Spar consist of 3 sections, a buoyant upper section or hard tank fitted with helical strakes, chains, and fairleads, a mid truss section with vertical and diagonal truss members and heave plates, and a lower cylindrical section known as the soft tank. A scaled model (1:40 Froude scale) shown in Figure 2 is tested in a model basin by towing.
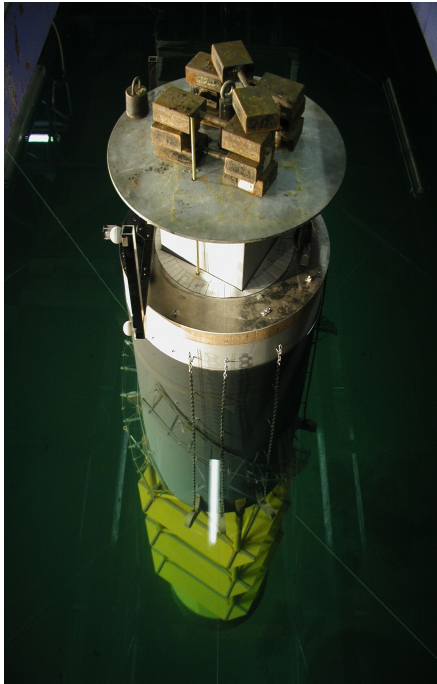

Figure 2: Truss Spar model in tow basin

Described in this section are properties of the model and conditions of the test. The diameter D of the Spar (hard tank and soft tank) is 741 mm and the tow tank depth is 5,400 mm. The roughness k on these hard and soft tanks are 0.333 mm ($\frac{k}{D}$ = 0.0004) and 3.33 mm ($\frac{k}{D}$ = 0.0045). The perimeter of the hard tank has 3 helical strake with 13% strake width (96.33 mm), a pitch of 4.53D, and wraps around 120º with a height of 1.51D.

The model is balanced and held in place with a liner mooring system. The system simulates inline and transverse stiffness to reflect the full scale mooring design. It has 4 lines with a spring stiffness of 40 N/m and a pretension of 36.6 N per line. The lines are attached to the bottom of the hard tank per the lengths and angles shown in Figures 3 and 4. The resulting inline stiffness k_x and transverse siffness k_y are 94.112 N/m and 91.613 N/m respectively from the static offset test.
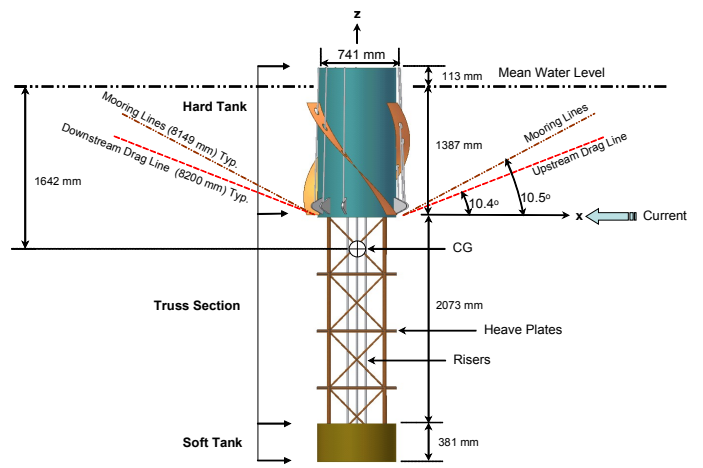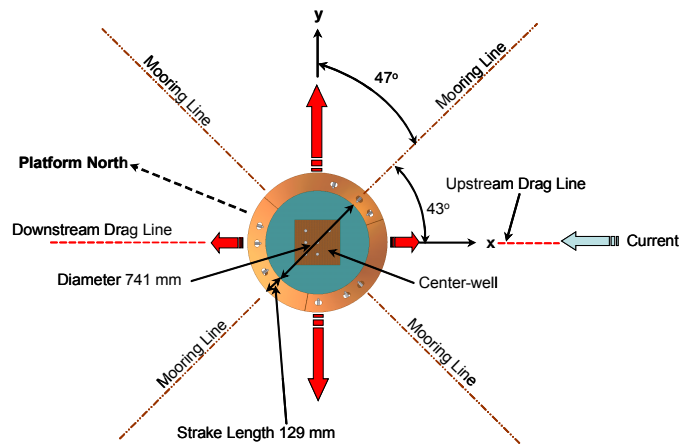

Figure 3: Truss Spar model side view

Figure 4: Truss Spar model top view

Drag lines are used to compensate for the drag due to current. These cable lines are tensioned using counterweights. These weights are proportionally moved to the upstream line by reducing weights on the downstream line as the towing speed increases to maintain the Spar within a central watch circle. Since the total weight remains the same, the effective transverse stiffness of these lines are constant and accounted in the design of the mooring system.

Other important model properties are:

- Mass of the model is 580 kg in water (not including water entrained in the centerwell)
- Center of gravity is 1,642 mm from the mean water line

The centerwell is a square section in the center of the hard tank (342 mm x 324 mm) and soft tank (320mm x 320mm) for risers to pass through shown in Figure 5. The total mass of the entrained water in the centerwell is 145 kg (114 kg for hard tank and 31 kg for soft tank). Hence the total mass of the system is 725 kg.

Table 2: Experimental results

Case	U (m/s)	$V_{R(N)}$	$V_{R(O)}$	Re	F_D (N)	F_U (N)	T_O (sec)	RMS Y/D	(Max –Min) / 2			Figures
									Y/D	X/D	Psi (deg)	
1	0.116	3.95	2.56	85692	73.847	88.999	16.4	0.010	0.037	0.020	0.059	8, 9
2	0.145	4.95	5.07	107386	69.424	93.422	25.9	0.025	0.071	0.027	0.090	10, 11
3	0.174	5.96	6.76	129298	63.374	99.472	28.7	0.048	0.106	0.024	0.124	12, 13
4	0.204	6.97	7.52	151209	56.815	106.031	27.3	0.077	0.192	0.038	0.235	14, 15
5	0.234	8.00	8.31	173554	49.036	113.810	26.3	0.128	0.367	0.068	0.564	16, 17
6	0.262	8.95	8.84	194163	41.003	121.843	25	0.122	0.282	0.047	0.692	18, 19
7	0.293	10.00	9.60	216942	29.055	133.791	24.3	0.146	0.303	0.060	0.675	20, 21

Note:
U   - Free stream current speed
$V_{R(N)}, V_{R(O)}$ - Reduced velocity ($U*T_N/D$, $U*T_O/D$) [calm water (N) and current (O)]
Re   - Reynolds number
T_O - Y/D mean measured oscillation period
F_D, F_U - Drag line tensions [downstream (D) and upstream (U)]
Y/D   - Transverse dimensionless amplitude
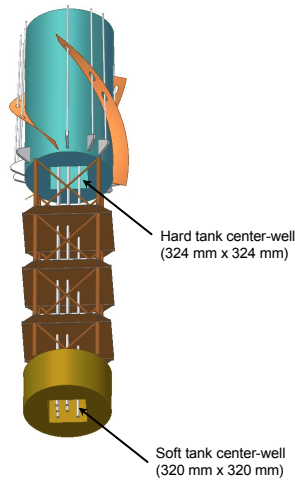X/D   - Inline dimensionless amplitude
Psi   - Yaw

Figure 5: Truss Spar model bottom-up view

Table 1: Free Decay Test

Motion	DOF	T_N (sec)
Surge	X	24.75
Sway	Y	25.32
Heave	Z	3.87
Roll	XX	8.70
Pitch	YY	8.60
Yaw	ZZ	5.02

The natural periods T_N listed in Table 1 are from a free decay test in calm water with the Spar oriented to receive current from 0°.

Figure 6: Experimental result configuration

The results presented in Table 2 are from currents in the 150° direction shown in Figure 6, the direction that gave the largest response. The water in the model basin has density and kinematic viscosity of 1,000 kg/m³ and 1.0e-6 m²/s.

CFD MODELING

CFD simulations including all the geometric details of the model test would be costly and so the model has to be simplified depending on the relative importance of various components to VIM response. The hard tank cylindrical section is the primary bluff body that causes VIM response due to vortex shedding and the strakes disrupts the vortex formation to reduces response.

For computational efficiency, the truss and soft tank sections are ignored in the CFD model, but inertia and drag contribution from these sections are included in the simulation using Morison formulation. Also, the hard tank centerwell and the appendages (chains and fairlead) are ignored. The entrained water mass in the centerwells (hard and soft tanks) and the mass of the appendages, truss section, and soft tank section are accounted in the total mass of the system. Figure 7 illustrates the model used for simulation ignoring the holes on the strakes.
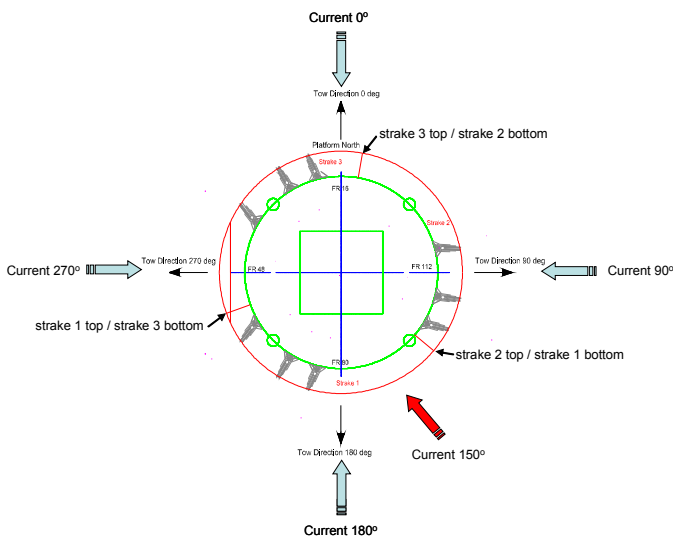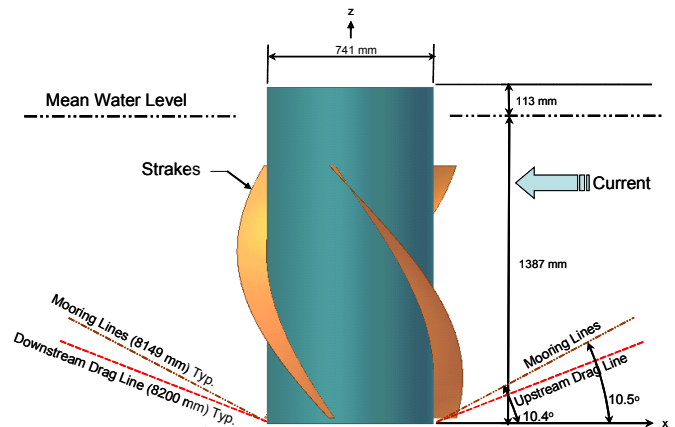

Figure 8: CFD modelling

Instead of modeling the 6 degrees of freedom (DOF) as in the experiment, only 2 degrees are modeled in surge x and

sway y. For any degree of freedom i, by double integrating the accelerations, the displacement d is

$$a_i = \frac{F_i}{m} \quad \rightarrow \quad d_i = \iint a_i \, dt \, dt$$

where F_i is the force and m is the total mass of model. The neglected truss section and soft tank are included in the simulation using Morison formulation as a user defined function. The Morison formulation which combines the inertial and drag terms (in Newtons) in x and y are

$$F_{x,morison} = -86.4(\ddot{x}) + 324.14(U - \dot{x})\sqrt{(U - \dot{x})^2 + \dot{y}^2}$$

$$F_{y,morison} = -86.4(\ddot{x}) - 324.14(\dot{x})\sqrt{(U - \dot{x})^2 + \dot{y}^2}$$

with U being the current in the x direction, $\dot{x}$ and $\dot{y}$ are Spar velocities, and $\ddot{x}$ and $\ddot{y}$ are Spar accelerations. The total force and moment in 2 DOF are

$$F_x = F_{x,hydro} + F_{x,morison} + F_{x,mooring} + F_{x,dragline}$$

$$F_y = F_{y,hydro} + F_{y,morison} + F_{y,mooring} + F_{y,dragline}$$

where subscripts *hydro*, *morison*, *mooring*, and *dragline* indicate the hydrodynamic, morison, mooring, and dragline contibutions.

An unstructured tetrahedral mesh is used for the simulations. A coarse mesh of 54,000 nodes is initially built to verify the model using case 5 in Table 2 and to compare the difference between LES and VMS methods. Once the model is verified, then a fine mesh with refinements zones shown in Figure 8 and 9 is built to run the cases in Table 2. There are no boundary layer elements and turbulence is accounted for by law of the wall in both meshes. The fine mesh has 460,000 nodes and 2,628,000 tetrahedral elements. The depth of the flow domain from the mean water level is 5,400 mm. The simulations are run for 600 seconds. The flow is initialized with a stationary Spar in the first 100 seconds before allowing 2 DOF motion.
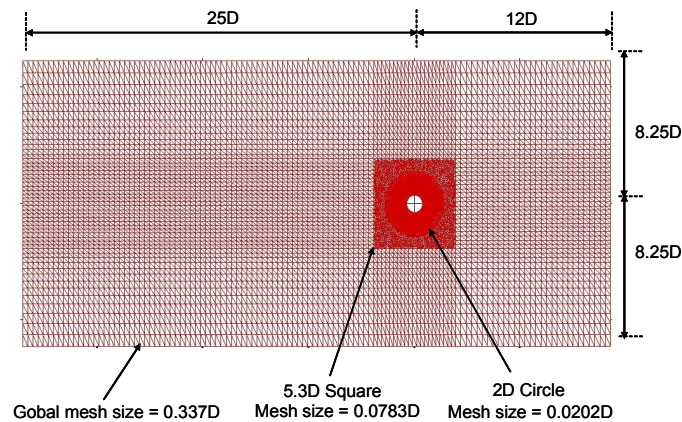

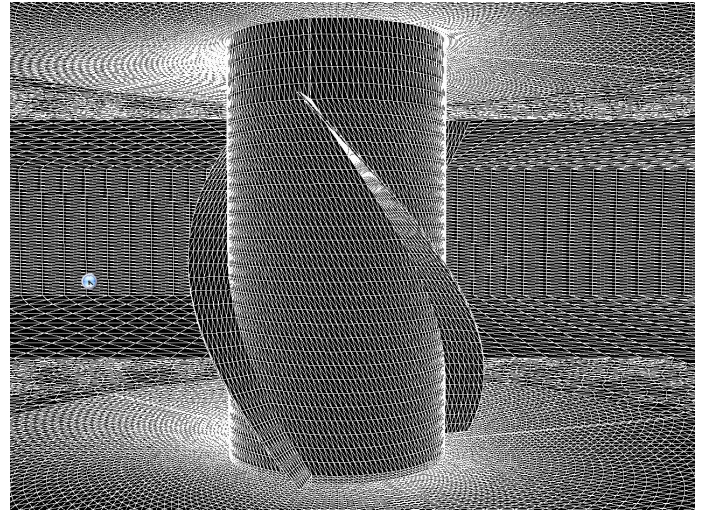Figure 9: Simulation flow domain and refinements

Figure 10: CFD model

The statistical result from 400 seconds, eliminating the first 33% of the transient record, are compared with the following experimental results in Table 2:

- RMS Y/D
- (Max Y/D – Min Y/D) / 2

(Max Y/D – Min Y/D) / 2 is not a good comparison of the response because maximum and minimum depends on the the length of the runs, however here it is compared only to shows trends.

CFD METHODS

The turbulence modeling considered in this paper are statistical law of the wall treatment of boundary layers, Smagorinsky LES model, and Variational Multiscale variant of the Smagorinsky LES model. The resolved turbulance scale aft of the Spar is 0.0202D. This turbulent viscosity is added on a micro scale and not on a macro scale.

Smagorinsky LES (LES)

The incompressible Navier-Stokes equations are given by,

$$\frac{\partial \boldsymbol{u}}{\partial t} + \nabla \cdot (\boldsymbol{u} \times \boldsymbol{u}) = -\frac{1}{\rho} \nabla P + \nabla \cdot \sigma$$

$$div \ \boldsymbol{u} = 0$$

where $\boldsymbol{u}$ is the velocity, P the pressure, ρ the density. The viscous stress tensor is define by:

$$\sigma_{ij} = \nu \left(2 \boldsymbol{S}_{ij} - \frac{2}{3} \boldsymbol{S}_{kk} \delta_{ij} \right)$$

where ν is the viscosity and

$$S_{ij} = \frac{1}{2}\left(\frac{\partial u_i}{\partial x_j} + \frac{\partial u_j}{\partial x_i}\right)$$

In order to introduce the basic LES model, it is necessary to assume discretization of the above Navier-Stokes equations on an unstructured tetrahedral mesh of a 3D Computational domain. We apply the model described in reference [3]. In the incompressible case

$$\frac{\partial \boldsymbol{u}}{\partial t} + \nabla \cdot (\rho \boldsymbol{u} \times \boldsymbol{u}) = -\frac{1}{\rho}\nabla P + \nabla \cdot (\sigma + \tau) \quad (1)$$

$$div\ \boldsymbol{u} = 0$$

with

$$\tau_{ij} = \nu_t \left(2\boldsymbol{S}_{ij} - \frac{2}{3}\boldsymbol{S}_{kk}\delta_{ij}\right)$$

$$S_{ij} = \frac{1}{2}\left(\frac{\partial \boldsymbol{u}_i}{\partial \boldsymbol{x}_j} + \frac{\partial \boldsymbol{u}_j}{\partial \boldsymbol{x}_i}\right)$$

$$\nu_t = (C_s \Delta)^2 |\boldsymbol{S}|$$

given

$$|\boldsymbol{S}| = \sqrt{2\boldsymbol{S}_{ij}\boldsymbol{S}_{ij}} \quad \text{with} \quad C_s = 0.1$$

and Δ denotes the local grid size. In this work, Δ is set to the volume of each tetrahedron T_l to the power of one third.

$$\Delta_i = Vol(T_l)^{\frac{1}{3}}$$

Combined with damping functions, the Smagorinsky LES model is able to predict boundary layers accurately with a high degree of mesh refinement in this layer. It is a costly option and not adequate for practical applications. An alternative approach is to equip the LES model with a statistical law of the wall model. In our work, this is accomplished by introducing a Reichardt type law of the wall, compatible with small and large y+ values.

LES-Variational Multi-Scale method (VMS)

The Variational Multi-Scale method has been introduced by Hughes and co-workers [2]. The purpose of this work is to compare the above LES model with a new version of the Variational Multi-Scale introduced by [3] for unstructured meshes.

To define the Variational Multi-Scale approach, we need to further define our numerical approximation by Mixed-Element-Volume method. The main novelty in VMS is a building of a coarse level made of large-scale nodes and corresponding large-scale basis functions. The set of large-scale basis function is complemented by fine-scale basis and tests functions (that we denote by ϕ').

The model filtering is applied by the previous Smagorinsky eddy viscosity, but this time, it involves only the fine-scales. For this, it is added to the equation governing the behavior of the fine-scales. This means that the term

$$\int_\Omega \tau' \nabla \Phi'\, d\Omega$$

is added to the momentum equation. We can write in short the global VMS formulation as follows (compare with Equation (1)):

$$\int_\Omega \frac{\partial \boldsymbol{u}}{\partial t} X_i\, d\Omega + \int_{\partial SupX_i} \boldsymbol{u} \times \boldsymbol{u}\, \boldsymbol{n}\, X_i\, d\Gamma + \int_{\partial SupX_i} \frac{1}{\rho} P\, \boldsymbol{n}\, X_i\, d\Gamma$$
$$+ \int_\Omega \sigma \nabla \Phi_i\, d\Omega + \int_\Omega \tau' \nabla \Phi_i'\, d\Omega = 0 .$$

Since the VMS model does not apply to large scale, the transfer of energy from small to large scale (and especially for flow separation) is damped to a lesser extent by the model.

CFD RESULTS

First a study with a coarse mesh of 54,000 nodes for case 5 ($V_{R(N)} = 8$) in Table 2 is performed to compare the results between LES and VMS. Figure 10 presents the motion comparison for these two methods. In contrast to VMS, LES under predicts the response.
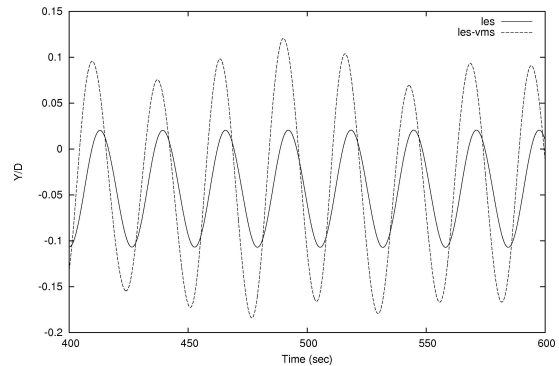
Figure 10: Scheme comparison using coarse mesh at $V_{R(N)} = 8$
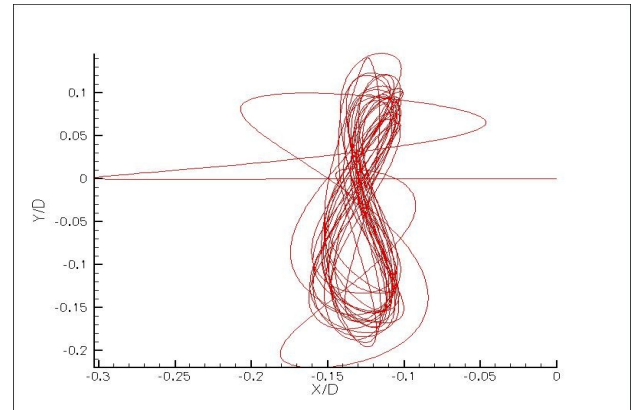
Figure 11: Coarse mesh Spar VIM response at $V_{R(N)} = 8$

The Spar VIM motion for the VMS simulation is shown in Figure 11, which assumes the traditional figure 8 response after the initial transient phase. Table 3 presents VMS comparison to experiment for the response. Even with a coarse mesh, the periods compared well. However, the RMS Y/D shows a 24% error and it is likely that this error is due to the nature of the coarse mesh. The (Max Y/D – Min Y/D) / 2 amplitude is about half of what was observed in the experiment.

Table 3: Coarse Mesh comparison at $V_{R(N)} = 8$

	Experiment	CFD
T_o	26.3 sec	26.4 sec
RMS Y/D	0.128	0.094
(Max Y/D – Min Y/D) / 2	0.367	0.168

Various finer meshes were investigated and what was important is to have enough elements along the strakes to capture the mixing layer well. The results presented here for the fine mesh described in the modeling section, took 20 hours on a 32 CPU 2 GHz Opteron cluster using a Gigabit network. The time step used is 0.04 seconds and the CFL number is 100. The comparison to experiments are presented in Figure 12 showing the relationship between freestream current (U), dimensional amplitude (Y/D), and reduced velocities ($V_{R(N)}, V_{R(O)}$).
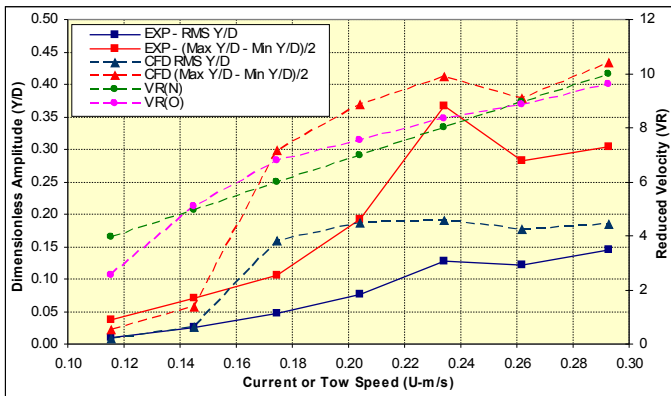

Figure 12: VMS in-line and transverse response

The dimensionless amplitude Y/D trend with respect to freestream current U are plotted with respect to the right axis, where the solid lines with squares represent experimental results and dashed lines with triangles represent CFD results. The other dashed lines with circular markers, plotted with respect to the left axis, represents the two different calculated reduced velocities, one in calm water $V_{R(N)}$ and the other with current $V_{R(O)}$.

CFD simulations does well when there is no response at $V_{R(N)}$ below 5, and when there is response above 8, even if they are sightly over predicted. However in the intermediate range between 5 and 8, the response is considerably over predicted. Compared to similar DES simulations [6], the VMS method compares better to the experimental results. The intermediate range need to be further studied to understand why it is so and what assumptions in the current CFD model need be improved upon. From experiments and DES CFD simulations it has been observed that including the chains and the holes will only increase the response. Since the primary Spar VIM response is in sway (transverse) and surge (in-line) the 2 DOF assumption is believed to have little impact changing the solution for the better. Thus we are left with one assumption, not explicitly modeling the truss and soft tank section. The Morison formulation used to neglect the truss and soft tank section was shown by the authors using a DES simulations to impact the prediction significantly. Further studies using the current VMS scheme will continue in this direction.

The Spar VIM response at $V_{R(N)} = 8$ are compared side by side between CFD on the left and experiment on the right in Figure 13. Although it is higher the similarity in response is evident. They both show a banana shape response compared to the classical figure 8 response predicted by the coarse mesh.
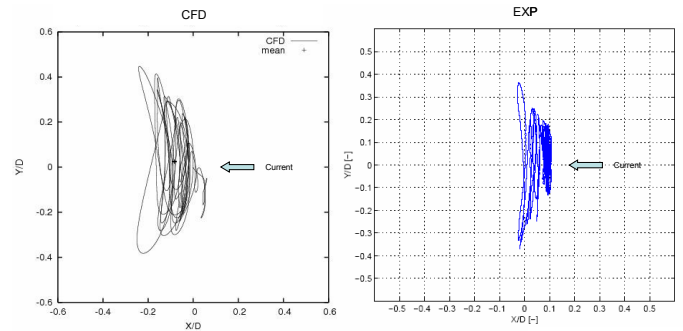

Figure 13: Fine mesh Spar VIM response at $V_{R(N)} = 8$

What is interesting in these simulations are the fact that the trends are being predict well and visualization of the flow as shown in Figure 14 provides a wealth of information about the behavior of strakes. This information could be used to better design strake configurations to mitigate VIM [7].
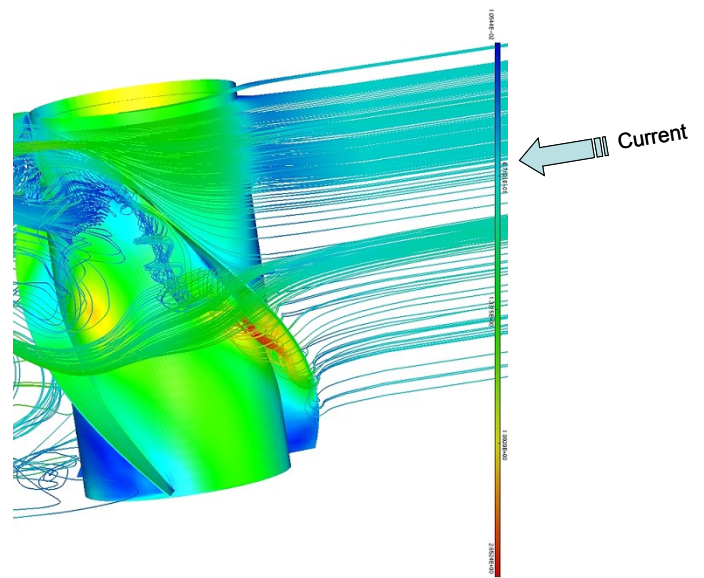

Figure 14: Streamlines being diverted by a strake for $V_{R(N)} = 10$

CONCLUSIONS

LES-Variational Multi-Scale (VMS) method is shown to better capture the VIM response of a model scale Truss Spar compared to LES based on a coarse mesh without explicit modeling of details such as chains, holes on strakes, fairleads, centerwell, risers, truss section, and soft tank. This approach couples integration of fluid forces with rigid body motion. The results obtained are somewhat consistent with several previous studies using DES [4][5]. The main difference however is that the simpler model better predicted the response overall using the VMS scheme. Even though the prediction are high in the intermediate reduced velocity range of 5 and 8, the results are rather encouraging. This study warrants continued investigation of a detail model to challenge the Morison formulation used in this study. In general, current and other authors have shown that CFD methods can effectively be used to predicted the VIM trend and understanding the flow through visualization can help achieve a better VIM mitigation device.

REFERENCES

[1] Blevins R.D., *Flow-Induced Vibration*, Van Nostrand Reinhold, New York, 1990.

[2] T.J.R. Hughes, L. Mazzei and K.E. Jansen, *Large eddy simulation and the variational multiscale method*, Comput. Vis. Sci., 3, 47, 2000.

[3] B. Koobus and C. Farhat, *A variational multiscale method for the large eddy simulation of compressible turbulent flows on unstructured mesh-application to vortex shedding*. Computer Methods in Applied Mechanics and Engineering, 193(15-16):1367-1383, 2004.

[4] Oakley, O., Constantinides, Y., Navarro, C. and Holmes, S., *Modeling Vortex induced Motions of spars In uniform and stratified flows*, Proceedings 24th International Conference on Offshore Mechanics and Arctic Engineering, OMAE2005-67238, Halkidiki, Greece, 2005.

[5] J. Halkyard, S. Sirnivas, S. Holmes, Y. Constatinides, O. Oakley, K. Thiagarajan, *Benchmarking of truss spar vortex induced motions derived from CFD with experiments*, Proceedings 24th International Conference on Offshore Mechanics and Arctic Engineering, OMAE2005-67238, Halkidiki, Greece, 2005.

[6] S.Atluri, J. Halkyard, S. Sirnivas, *CFD Simulation Of Truss Spar Vortex-Induced Motion*, Proceedings 25th International Conference on Offshore Mechanics and Arctic Engineering, OMAE2006-92400, Hamburg, Germany, 2006.

[7] J. Halkyard, S.Atluri, S. Sirnivas, *Truss Spar Vortex Induced Motions: Benchmarking Of CFD And Model Tests*, Proceedings 25th International Conference on Offshore Mechanics and Arctic Engineering, OMAE2006-92673, Hamburg, Germany, 2006.